

# Characterization of SiO<sub>2</sub> and TiO<sub>2</sub> films prepared using rf magnetron sputtering and their application to anti-reflection coating

Sang-Hun Jeong<sup>a</sup>, Jae-Keun Kim<sup>b</sup>, Bong-Soo Kim<sup>a</sup>, Seok-Ho Shim<sup>a</sup>,  
Byung-Teak Lee<sup>a,\*</sup>

<sup>a</sup>*Department of Materials Science and Engineering, Photonic and Electronic Thin Film Laboratory, Chonnam National University, 300 Yongbong-Dong, Buk-Gu, Kwangju 500-757, Republic of Korea*

<sup>b</sup>*Department of Physics, Chonnam National University, 300 Yongbong-Dong, Buk-Gu, Kwangju 500-757, Republic of Korea*

Received 30 March 2004; received in revised form 25 June 2004; accepted 28 June 2004

## Abstract

Preparation of TiO<sub>2</sub> and SiO<sub>2</sub> films for optical applications was attempted using conventional rf magnetron sputtering in the sputtering ambient with various O<sub>2</sub>/Ar+O<sub>2</sub> ratios and at substrate temperatures between room temperature and 400 °C. X-ray photoelectron spectroscopy (XPS) and optical spectroscopy investigations indicated that oxygen addition in the sputtering ambient was essential for growing TiO<sub>2</sub> films with stoichiometric compositions and good transmittance, while SiO<sub>2</sub> films had a stoichiometric composition of O/Si ratio=2.1–2.2 and were highly transparent in the visible wavelength region, independent of gas composition in the growing ambient. It was also identified from scanning electron microscope (SEM), atomic force microscope (AFM) and Fourier transform infrared spectroscopy (FTIR) measurements that the structural characteristics of both TiO<sub>2</sub> and SiO<sub>2</sub> films were significantly improved with O<sub>2</sub> addition in the sputtering ambient, showing smoother surface morphologies and higher resistances to water absorption when compared with films grown without O<sub>2</sub> addition. Heating of the substrate between 200 and 400 °C considerably increased the refractive index of TiO<sub>2</sub> layers, resulting in dense structures along with an improvement of crystallinity. For optical applications, AR coatings composed of 2–4 multi-layers on glass were designed and manufactured by stacking in turn the SiO<sub>2</sub> and TiO<sub>2</sub> films at room temperature and O<sub>2</sub>/Ar+O<sub>2</sub>=10%, and the performance of the produced coatings was compared with simulation results.

© 2004 Elsevier Ltd. All rights reserved.

**Keywords:** TiO<sub>2</sub> film; SiO<sub>2</sub> film; rf magnetron sputtering; AR coating

\*Corresponding author. Tel.: +82-62-530-1696; fax: +82-62-530-1699.

E-mail address: [photon@chonnam.ac.kr](mailto:photon@chonnam.ac.kr) (B.-T. Lee).

## 1. Introduction

TiO<sub>2</sub> and SiO<sub>2</sub> films have various applications as dielectric layers for electronic devices and as layers with low-and high-refractive index in optical layer systems, such as antireflective coatings and optical filters. In addition, TiO<sub>2</sub> films have attracted much interest for use in photocatalysis and photochemical solar cells [1,2] and more recently, it was found that titanium compounds are biocompatible, making them attractive as an implant material. Therefore, many studies of the preparation of TiO<sub>2</sub> and SiO<sub>2</sub> films have been carried out using various deposition procedures [3–6].

The usual methods employed for forming SiO<sub>2</sub> and TiO<sub>2</sub> films involve high temperature processes like thermal oxidation and chemical vapour deposition (CVD). However, high-temperature processing results in junction degradation and has a shortcoming that substrates with low melting points like glasses and polycarbonates, which are mainly utilized in optical application, cannot be used.

Despite the low deposition rate, reactive sputtering has been considered as a useful technique to deposit the high quality dielectric films such as SiO<sub>2</sub> and TiO<sub>2</sub> at a low substrate temperatures (<100 °C), because the sputter process can be easily controlled and the deposited layers show good adhesion as well as good coating uniformity. Even though many reports on preparation of SiO<sub>2</sub> and TiO<sub>2</sub> films using sputter methods exist [7–9], there are not many reports on full characterization of both SiO<sub>2</sub> and TiO<sub>2</sub> films grown by reactive sputtering and, further, the production of optical coatings using these films is currently of significant interest.

In this study, we report on the preparation of TiO<sub>2</sub> and SiO<sub>2</sub> films with good optical and structural properties applicable to optical coatings using a conventional rf magnetron sputter system and on their application for the production of antireflection coatings. For this purpose, the films deposited in Ar/O<sub>2</sub> mixture with different O<sub>2</sub>/Ar+O<sub>2</sub> ratios and at substrate temperatures between room temperature and 400 °C were extensively characterized using various analytical techniques, and AR coatings comprised of SiO<sub>2</sub>/

TiO<sub>2</sub> multi-layers on glass were designed and manufactured under optimal conditions. The performance of these coatings was evaluated by comparing with simulation results.

## 2. Experiment

A conventional rf magnetron sputter system was used to deposit SiO<sub>2</sub> and TiO<sub>2</sub> films from TiO<sub>2</sub> and SiO<sub>2</sub> ceramic targets (99.999% purity) with a diameter of 0.1 m. Si(1 0 0) wafers and float glasses were utilized as substrates for structural and optical characterization, respectively. The process chamber was evacuated below  $7 \times 10^{-6}$  mbar prior to deposition and all depositions were carried out in Ar/O<sub>2</sub> mixture with various O<sub>2</sub>/Ar+O<sub>2</sub> ratios between 0% and 30% under a constant working pressure of  $7 \times 10^{-3}$  mbar. Substrate temperature was varied from no deliberate heating to 400 °C and sputtering of the target was performed at a high power of 250 W, owing to the low sputtering yields of both TiO<sub>2</sub> and SiO<sub>2</sub> ceramic targets. A distance between target and substrate was maintained at 50 mm for all depositions.

Optical characteristics of the deposited films were examined using an ex-situ ellipsometer (J. A. Woollam VUV-VASE VU-302) with measurements at a wavelength of 632.8 nm and by optical spectra measurements using UV–VIS–NIR spectrophotometer (Hitachi U-4000). Crystallinity and orientation of the films were assessed with the Philips X'Pert PRO-MRD high-resolution 4-crystal triple axis X-ray diffractometer (HR-XRD), using a Cu K $\alpha$  radiation. The chemical state, structure, and composition of the films were checked through X-ray photoelectron spectroscopy (XPS) measurements (Perkin–Elmer PHI ESCA 5500 system) and a Fourier transform infrared spectroscopy (FTIR). A JEOL JEM 2000FX transmission electron microscope (TEM), field emission scanning electron microscope (FESEM) (Hitachi S-4700), and a Digital Instruments Multi-Mode atomic force microscope (AFM) were also employed to observe microstructure of the samples.

Finally, AR coatings composed of multi-stack SiO<sub>2</sub> and TiO<sub>2</sub> films on glass were produced at

optimal growth conditions and the performance was estimated using a spectrophotometer and compared with simulation results.

### 3. Results and discussion

#### 3.1. Characterization

Fig. 1 shows the thickness of the SiO<sub>2</sub> and TiO<sub>2</sub> films deposited on Si(100) substrates, at various O<sub>2</sub>/Ar+O<sub>2</sub> ratios for 30 min as a function of O<sub>2</sub>/Ar+O<sub>2</sub> ratio. Though substrates were not heated deliberately, substrate temperature during deposition was maintained at 70–80 °C due to radiative heating by energetic particles incident on the substrate. The deposition rate of the films decreased abruptly with a small amount of O<sub>2</sub> addition and this reduction in deposition rate by O<sub>2</sub> addition may be due to the decrease of sputtering yield caused by a mass difference between Ar and O<sub>2</sub>. It is also considered that the abrupt reduction in deposition rate depending on the growing ambient can be related to a phase change of the target surface during deposition, i.e., when sputtered in pure Ar ambient, the surfaces of TiO<sub>2</sub> and SiO<sub>2</sub> targets can be changed to Ti- or Si-rich phases owing to the preferential sputtering of oxygen, resulting in higher sputtering yield, while during sputtering in ambient containing oxygen,

target surface can maintain a more oxidized phase, resulting in lower sputtering yield. In fact, as shown in Fig. 1, the reduction in the deposition rate is more severe in the case of TiO<sub>2</sub> and this is understood to be due to the large mass difference between Ti and O.

The effects of sputtering-gas composition on the film composition and the chemical state were investigated by XPS measurement. All XPS spectra were taken after 50 s Ar<sup>+</sup> sputtering to eliminate surface contamination and to minimize disturbance of the layer due to preferential sputtering. Ti2p XPS spectra for TiO<sub>2</sub> films grown with and without O<sub>2</sub> addition are shown in Fig. 2. In Fig. 2(a), Ti2p XPS spectrum for TiO<sub>2</sub> film prepared in pure Ar ambient can be deconvoluted into five peaks. The peaks at 455.5, 457.1 and 460.9 eV are assigned to Ti<sup>2+</sup>2p<sub>3/2</sub>, Ti<sup>3+</sup>2p<sub>3/2</sub>, and Ti<sup>3+</sup>2p<sub>1/2</sub> states in TiO and Ti<sub>2</sub>O<sub>3</sub>, respectively

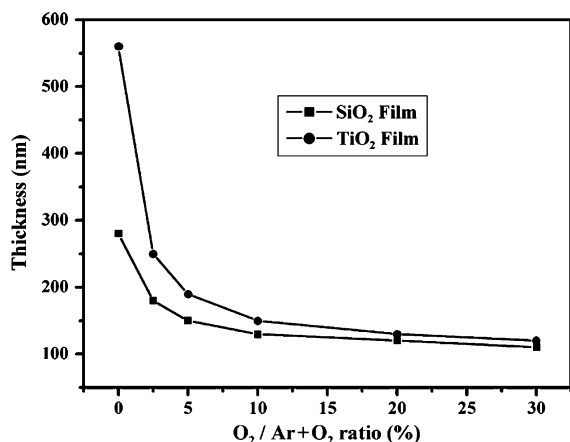


Fig. 1. Thicknesses of TiO<sub>2</sub> and SiO<sub>2</sub> films deposited on Si(100) substrates for 30 min at various O<sub>2</sub>/Ar+O<sub>2</sub> ratios.

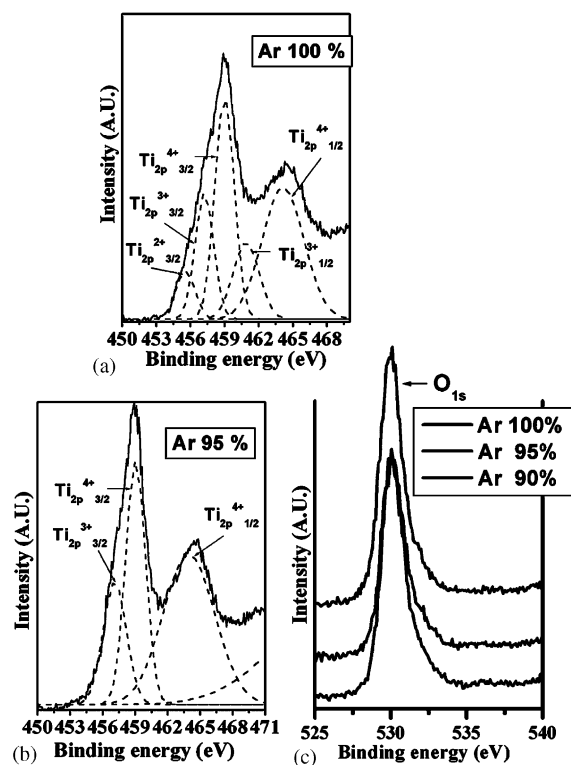


Fig. 2. Ti<sub>2p</sub> binding energy spectra deconvoluted using a Gaussian distribution function for TiO<sub>2</sub> films deposited at O<sub>2</sub>/Ar+O<sub>2</sub> ratios of (a) 0% and (b) 5%, and (c) O<sub>1s</sub> binding energy spectra for the same films.

and two peaks at 459 and 464.6 eV correspond to  $\text{Ti}2p_{3/2}$  and  $\text{Ti}2p_{1/2}$  binding energies in  $\text{TiO}_2$ , respectively. In Fig. 2(b),  $\text{Ti}2p$  XPS spectrum for  $\text{TiO}_2$  films grown with  $\text{O}_2$  addition show only an additional peak at 457.1 eV due to the  $\text{Ti}^{3+}2p_{3/2}$  in the  $\text{Ti}_2\text{O}_3$ , as well as the  $\text{Ti}^{4+}2p_{3/2}$  and  $\text{Ti}^{4+}2p_{1/2}$  peaks in the  $\text{TiO}_2$  [5,10]. As depicted in Fig. 2(c), the  $\text{O}1s$  core-level spectra for the same films show only a peak centered at 530 eV, which can be assigned to all  $\text{O}1s$  states in  $\text{TiO}_2$ ,  $\text{TiO}$ , and  $\text{Ti}_2\text{O}_3$  [11]. In addition, the ratio of oxygen to titanium ( $\text{O}/\text{Ti}$ ) in the films calculated from XPS spectra ranged from 1.65 at  $\text{O}_2/\text{Ar} + \text{O}_2 = 0\%$ , 1.93 at  $\text{O}_2/\text{Ar} + \text{O}_2 = 5\%$ , to 1.95 at  $\text{O}_2/\text{Ar} + \text{O}_2 = 10\%$ , indicating that the film stoichiometry was significantly improved with  $\text{O}_2$  addition in the sputtering ambient.

This result can be understood from the following discussion. During sputter deposition of the  $\text{TiO}_2$  target by Ar ion bombardment, the bombarded target surface can be changed to metal rich compared with the original surface, due to oxygen preferential sputtering and consequently, the composition in the deposited film also becomes metal rich, while with supply of oxygen, reduction of target surface to  $\text{TiO}_{2-x}$  is limited and  $\text{TiO}$  in film and/or on target surface is transformed to  $\text{Ti}_2\text{O}_3$  or  $\text{TiO}_2$  because  $\text{TiO}$  which has a relatively low heat of formation, easily reacts with the surrounding oxygen [12].

Fig. 3 shows XPS binding energy spectra of  $\text{Si}2p$  and  $\text{O}1s$  states for  $\text{SiO}_2$  films grown with and without  $\text{O}_2$  addition. All the  $\text{Si}2p$  and  $\text{O}1s$  spectra show only peaks centered at 103.5 and 533.1 eV corresponding to  $\text{Si-O}$  bonds, respectively. Also, the  $\text{O}/\text{Si}$  ratio calculated from XPS spectra ranged between 2.1 and 2.2, which means that the  $\text{SiO}_2$  films grown in this work were fully oxidized, independent of gas composition in the growing ambient.

The refractive index of  $\text{SiO}_2$  and  $\text{TiO}_2$  films measured using an ellipsometer at a wavelength of 632.8 nm is plotted in Fig. 4 as a function of the  $\text{O}_2/\text{Ar} + \text{O}_2$  ratio. In the case of  $\text{SiO}_2$  films, the film grown in pure Ar ambient had a lower index of 1.445 but the refractive indices of the films deposited with  $\text{O}_2$  addition were distributed near to 1.46, which is typical for  $\text{SiO}_2$  film. The lower

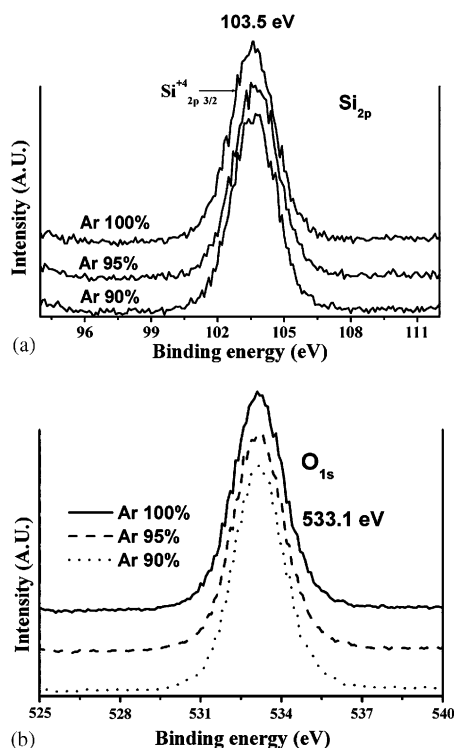


Fig. 3.  $\text{Si}2p$  and  $\text{O}1s$  binding energy spectra taken from  $\text{SiO}_2$  films deposited at  $\text{O}_2/\text{Ar} + \text{O}_2$  ratios of 0%, 5%, and 10%.

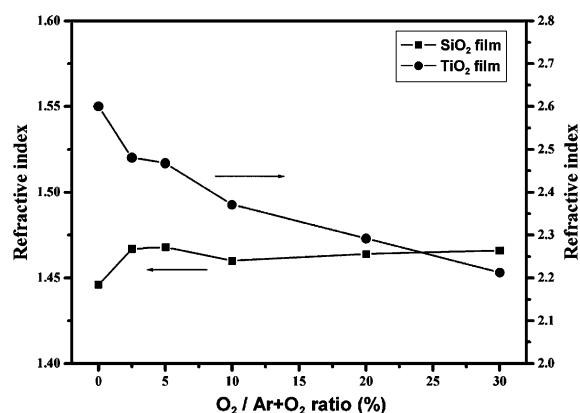


Fig. 4. Variation of refractive index of  $\text{TiO}_2$  and  $\text{SiO}_2$  films as a function of the  $\text{O}_2/\text{Ar} + \text{O}_2$  ratio.

refractive index of the  $\text{SiO}_2$  film prepared in pure Ar ambient can be due to the porous structure with a low packing density as will be discussed in

FTIR analysis. In the case of  $\text{TiO}_2$  films, the film grown in pure Ar showed a higher index value of 2.63, while with  $\text{O}_2$  addition, the refractive index gradually decreased from 2.481 at  $\text{O}_2/\text{Ar} + \text{O}_2$  ratio = 2.5%, 2.38 at  $\text{O}_2/\text{Ar} + \text{O}_2$  ratio = 10%, to 2.22 at  $\text{O}_2/\text{Ar} + \text{O}_2$  ratio = 30%.

Fig. 5 shows optical transmittances of the  $\text{TiO}_2$  and  $\text{SiO}_2$  films prepared at various  $\text{O}_2/\text{Ar} + \text{O}_2$  ratios. All the  $\text{SiO}_2$  films and  $\text{TiO}_2$  films grown in the ambient containing  $\text{O}_2$  were highly transparent but only  $\text{TiO}_2$  film grown in pure Ar showed a considerably lower transmittance. Also, the sum of reflectance (data not shown) and transmittance for all the  $\text{SiO}_2$  films and  $\text{TiO}_2$  films grown in the ambient containing  $\text{O}_2$  was nearly unity, 1. On the contrary, the  $\text{TiO}_2$  film grown in pure Ar showed a value below 0.9, indicating a considerable optical loss by optical absorption originating from Ti-rich composition as identified from XPS analysis. This

dependence of the refractive index and optical transmittance on the sputtering ambient observed from the  $\text{TiO}_2$  films implies that the film stoichiometry is improved with  $\text{O}_2$  addition, while a large amount of  $\text{O}_2$  addition can reduce the packing density of the film, forming porous films. Similar behaviour of refractive index versus oxygen mole fraction for  $\text{TiO}_2$  layers has been found for mid-frequency sputtering using a double magnetron arrangement [13].

The film microstructure was also investigated through SEM and AFM observations. Fig. 6 represents (a) SEM plan-view images and (b) root mean square (RMS) roughness for the  $\text{SiO}_2$  and  $\text{TiO}_2$  films as a function of  $\text{O}_2/\text{Ar} + \text{O}_2$  ratio in the growing ambient. It is observed in Fig. 6 that surface morphology is more smoothed and the size of grains forming the film decreases with  $\text{O}_2$  addition. This structural variation is more distinctive in  $\text{TiO}_2$  layers and might be beneficial to optical application since a smaller grain size and a smoother surface can reduce optical loss by scattering.

FTIR is also a useful technique to obtain the structural information and the chemical state of the  $\text{SiO}_2$  film. IR absorption spectra of the  $\text{SiO}_2$  films deposited at various  $\text{O}_2/\text{Ar} + \text{O}_2$  ratios are depicted in Fig. 7. These spectra were normalized to the same film thickness for relative comparison. In wide-range IR spectra shown in Fig. 7(a), the H–OH and Si–OH absorption bands having a close relation with water absorption are observed at  $3400$  and  $3650\text{ cm}^{-1}$ , as well as the three characteristic absorption bands of  $\text{SiO}_2$  near  $450$  (rocking),  $815$  (bending), and  $1060\text{ cm}^{-1}$  (stretching) [14]. The intensity of these OH and Si–OH absorption bands reduces with  $\text{O}_2$  addition and this trend is further clear in the high resolution IR spectra spanning the region  $2700\text{--}4000\text{ cm}^{-1}$  as shown in Fig. 7(b). In general, O–H-related bands can be due to the incorporation of hydrogen in films during deposition and water absorption by exposure to air after deposition. In the present study, it is evaluated that the higher intensity of the O–H and Si–OH absorption bands of the  $\text{SiO}_2$  film grown in pure Ar can be related to water absorption in the film, which means that the film structure is more porous [15] and the lower

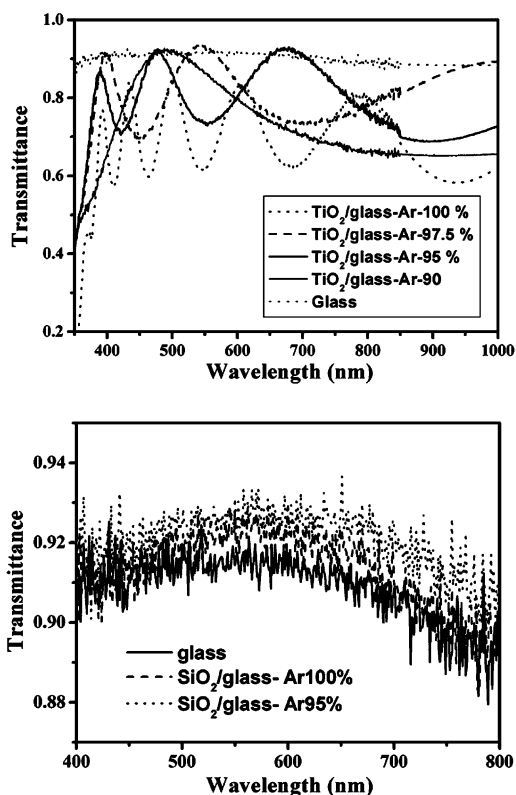


Fig. 5. Transmittance spectra of  $\text{TiO}_2$  and  $\text{SiO}_2$  films prepared at various  $\text{O}_2/\text{Ar} + \text{O}_2$  ratios.



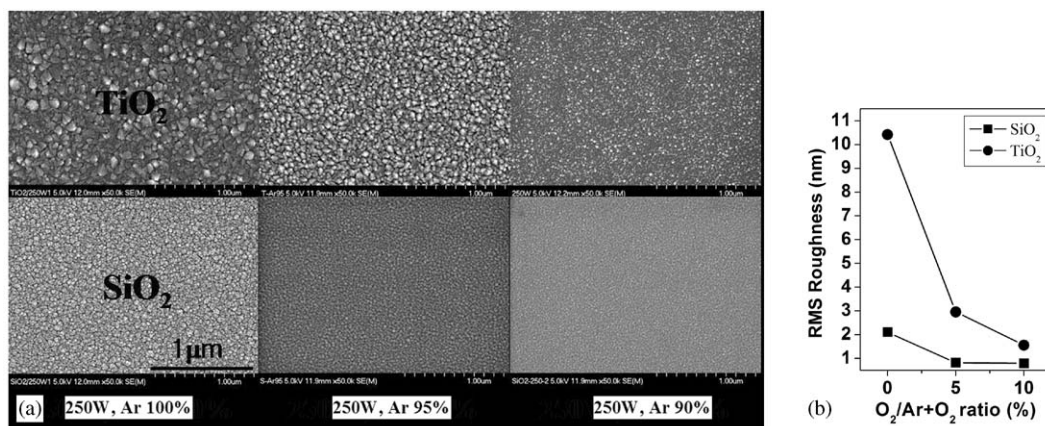


Fig. 6. (a) SEM plan-view images and (b) RMS roughness for SiO<sub>2</sub> and TiO<sub>2</sub> films prepared at O<sub>2</sub>/Ar + O<sub>2</sub> ratios of 0%, 5%, and 10%.

refractive index of this film may be an indicator of porosity.

It is also noted in a high-resolution IR spectra spanning the region 820–1300 cm<sup>-1</sup> plotted in Fig. 7(c) that with O<sub>2</sub> addition, the frequency of Si–O stretching mode ( $\nu_s$ ) slightly shifts to the lower frequency from 1065 to 1058 cm<sup>-1</sup>, and its full-width half maximum (FWHM) decreases. According to the central force model proposed by Sen and Thorpe [16], the higher frequency and the wider FWHM of the Si–O–Si stretching mode mean the larger Si–O–Si bond angle, this larger Si–O–Si bond angle has been recognized as a direct indicator of Si–O–Si bond relaxation in a SiO<sub>2</sub> network accompanied by lower density and lower refractive index [17].

It is desirable that the optical films have a hydrophilic property, because water absorption in the film can result in a shift of optical spectra by inducing a localized variation in refractive index and as a result, in the significant performance degradation of an optical system composed of multi-layers.

Growth temperature is also an important parameter, which can influence the microstructure and as a result the optical characteristics of the deposited films. Fig. 8 shows (a) XRD patterns, (b) TEM cross-sectional images, and (c) the variation of refractive index for the TiO<sub>2</sub> layers grown on silicon at temperature range from no heating to 400 °C and O<sub>2</sub>/Ar + O<sub>2</sub> = 10%. XRD measurement

using  $\theta$ – $2\theta$  scan mode indicates an improvement of film crystallinity and a variation of film structure from amorphous consisted of the micro-crystalline grains to polycrystalline anatase phase with increasing substrate temperature. TEM cross-sectional images also confirmed the variation of film structure towards a more dense and crystalline structure with growth temperature. In Fig. 8(c), the refractive index steeply rises from 2.38 to 2.58 with increasing substrate temperature from ambient temperature to 200 °C and then slightly increase to 2.61 at 400 °C. This index value is high, which is comparable to that of rutile phase TiO<sub>2</sub>, 2.7, though these TiO<sub>2</sub> films had an anatase phase as indicated in XRD patterns [18]. In contrast, it is also mentioned in the case of SiO<sub>2</sub> films that a discernable variation of structural and optical characteristics depending on the growth temperature was not observed.

### 3.2. Antireflective (AR) coatings

Antireflective coatings on glass are of essential importance in optical systems since the reflectance of a glass substrate is about 8.5%.

In general, narrow-band AR coatings comprise two layers with a structure of Sub/HL/air where H denotes a high-index material, L denotes a low-index material, and Sub denotes a substrate. It will give an antireflective property for one wavelength and thus, the reflection curve is V-shaped where

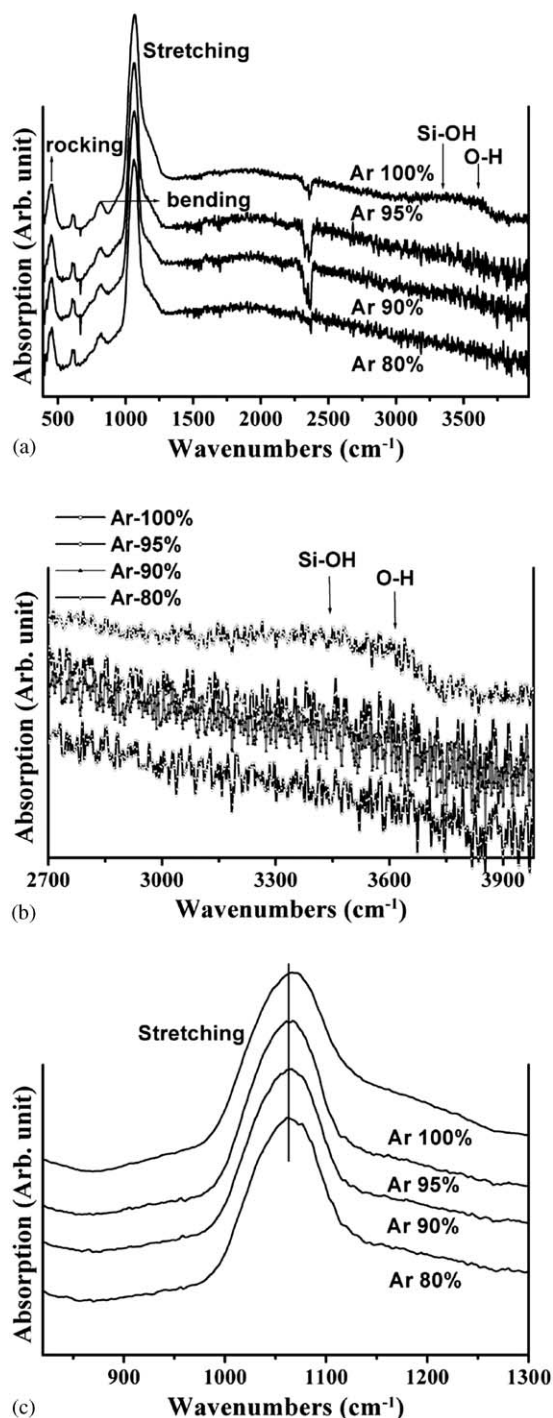


Fig. 7. (a) Wide range IR spectra and (b) high resolution IR spectra spanning the region 2700–4000 cm<sup>-1</sup>, and (c) high resolution IR spectra in the region 820–1300 cm<sup>-1</sup> obtained from SiO<sub>2</sub> films prepared at various O<sub>2</sub>/Ar + O<sub>2</sub> ratios.

the bottom is the reference wavelength. V-coats are not good for the AR coating in the visual range, owing to narrow bandwidth. A structure of Sub/MHL/air is needed to achieve antireflective property in a broad wavelength region where M denotes middle-index material. However, the refractive index of the middle-index material has to be a certain value and it is not convenient to search for such a material. Furthermore, at a production site, it is more preferable to use a fewer number of materials. Therefore, a four-layer antireflective coating with a structure of Sub/HLHL/air is often utilized.

In this work, to acquire antireflective properties in the visible wavelength region between 400 and 700 nm, a two-layer AR coating with a structure of glass/TiO<sub>2</sub>/SiO<sub>2</sub> and a four-layer AR coating with a structure of glass/TiO<sub>2</sub>/SiO<sub>2</sub>/TiO<sub>2</sub>/SiO<sub>2</sub> were designed and actually fabricated on a glass substrate with a refractive index of 1.54. AR coatings were designed for the reference wavelength of 500 nm. The main parameters for fabrication and design of AR coatings are the refractive index, extinction coefficient, and the film thickness of each layer. The refractive indices were chosen as 2.38 and 1.46, respectively, which are the refractive indices of the TiO<sub>2</sub> and SiO<sub>2</sub> films prepared at O<sub>2</sub>/Ar + O<sub>2</sub> ratio = 10% because the SiO<sub>2</sub> and TiO<sub>2</sub> films with properties suitable for optical application could be obtained at this condition, as described in the previous section. It was also assumed that the extinction coefficient was 0 since the optical loss or absorption was negligible in the films grown at this condition. The optimal thickness of each layer was simulated using Thin Film Calculation Software before the production of AR coatings. The thicknesses of the produced coatings were determined by means of an ex-situ spectroscopic ellipsometer.

The measured reflectance of the fabricated two-layer AR coating is presented in Fig. 9 together with theoretically simulated reflectance, and the desired sample geometry is shown in the inset. It is found in this figure that though the thickness of each layer slightly deviated from the desired thickness of the layer stack, the measured reflectance agrees well with the simulated reflectance.

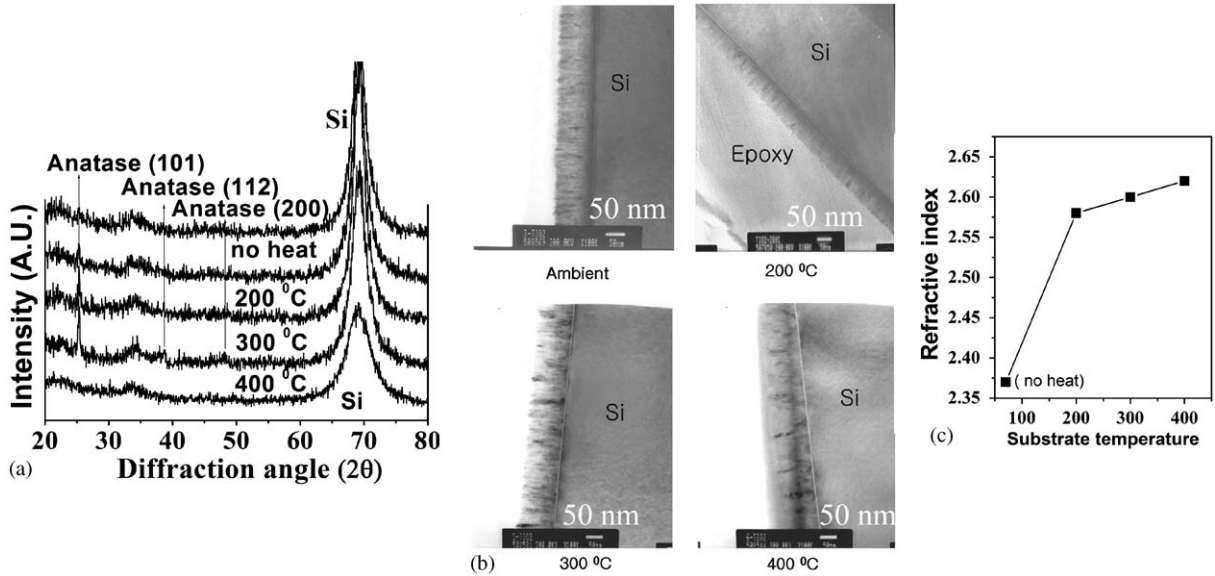


Fig. 8. (a) XRD patterns (including XRD pattern of bare silicon), (b) TEM cross-sectional images, and (c) the variation of refractive index for the TiO<sub>2</sub> layers grown on silicon at temperature range from no heat to 400 °C and O<sub>2</sub>/Ar + O<sub>2</sub> = 10%.

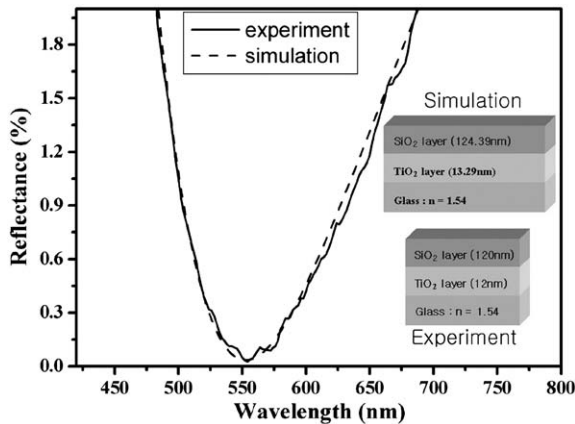


Fig. 9. Theoretical and experimental reflectance spectra of the two-layer AR coating. Inset: designed and fabricated structures of the two-layer AR coating.

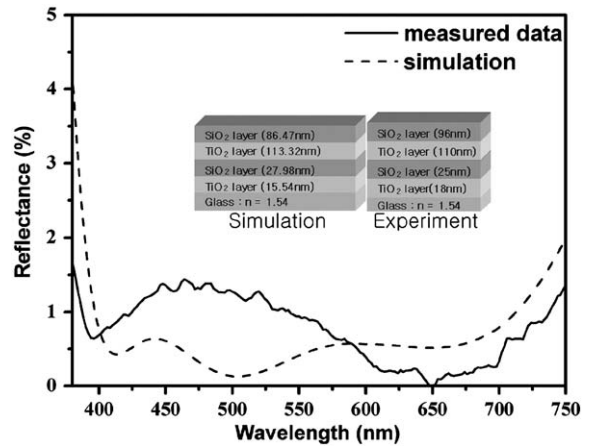


Fig. 10. Theoretical and experimental reflectance spectra of the four-layer AR coating. Inset: designed and fabricated structures of the four-layer AR coating.

Fig. 10 shows the measured reflectance and the theoretically simulated reflectance of a four-layer AR coating. The layer structures are shown in the inset of Fig. 10. The reflectance spectra of a four-layer AR coating exhibited a considerable discrepancy with the theoretical result, showing higher average reflectance in the region of

400–700 nm. This deviation between the theoretical and experimental results for a four-layer AR coating may result from a discrepancy of thickness of each layer in the AR coating, because optical interference at interfaces is more serious as the number of the stacked layers increases. For the



fabrication of multi-layer optical coatings with a high performance, more precise control over the layer thickness is necessary and this can be achieved through real-time monitoring using an in-situ spectroscopic ellipsometer.

#### 4. Conclusions

In this paper, preparation of  $\text{TiO}_2$  and  $\text{SiO}_2$  films for optical applications has been attempted using conventional rf magnetron sputtering in the sputtering ambient with various  $\text{O}_2/\text{Ar} + \text{O}_2$  ratios and growth temperatures in the range between no deliberate heating and  $400^\circ\text{C}$ .

It is suggested from the experimental results that small amounts of  $\text{O}_2$  addition in the growing ambient is necessary for depositing the  $\text{TiO}_2$  and  $\text{SiO}_2$  films having the compositional, structural, and optical characteristics suitable for optical application including the stoichiometric composition, good optical transmittance, smooth surface morphology, and strong resistance to moisture absorption. It is also noticeable in the case of  $\text{TiO}_2$  films that substrate heating to  $400^\circ\text{C}$  resulted in a densification of film structure and an improvement of film crystallinity along with a higher refractive index comparable to that of rutile  $\text{TiO}_2$ .

The two-layer and four-layer AR coatings were manufactured by stacking  $\text{SiO}_2$  and  $\text{TiO}_2$  films in turn on glass using rf magnetron sputtering in an ambient of  $\text{O}_2/\text{Ar} + \text{O}_2 = 10\%$ . The reflectance of the two-layer AR coating was in a good agreement with the simulated result while the reflectance of four-layer AR coating showed a slightly higher reflectance compared with the simulated result. It is evaluated that the deviation between the theoretical and experimental results may be due to a discrepancy of thickness of each layer. Thus,

more exact control of the layer thickness is essential for improving the performance of the AR coating.

#### Acknowledgements

This work was supported by Korean Ministry of Science & Technology through the National Research Laboratory program.

#### References

- [1] Graetzel M. Comments Inorg Chem 1991;12:93.
- [2] Hanawa T, Ota M. Appl Surf Sci 1992;55:263.
- [3] Battiston GA, Gerbasi R, Gregori A, Porchia M, Cattarin S, Rizzi GA. Thin Solid Films 2001;371:126.
- [4] Martinet C, Paillard V, Gagnaire A, Joseph J. J Non-Crystal Solids 1997;216:77.
- [5] Lee C, Zheng Z, Fuming Zhang, Yang S, Wang H, Chen L, Feng Zhang, Wang X, Liu X. Nucl Instrum Methods Phys Res B 2000;169:21.
- [6] Wen-Fa Wu, Bi-Shiou Chiou. Appl Surf Sci 1996;99:237.
- [7] Seifarth H, Schmidt JU, Grotzschel R, Klimenkov M. Thin Solid Films 2001;389:108.
- [8] Zheng SK, Wang TM, Xiang G, Wang C. Vacuum 2001;62:361.
- [9] Billard A, Merces D, Perry F, Frantz C. Surf Coat Technol 1999;116–119:721.
- [10] Ohsaki H, Tachibana Y, Mitsui A, Kamiyama T, Hayashi Y. Thin Solid Films 2001;392:169.
- [11] Sayers CN, Armstrong NR. Surf Sci 1978;77:301.
- [12] Jang HK, Whangbo SW, Kim HB, Lee YS, Lyo IW, Whang CNJ. Vac Sci Technol A 2000;18(3):917.
- [13] Bräuer G, Szczyrbowski J, Teschner G. Surf Coat Technol 1997;94–95:658–62.
- [14] Theil JA, Tsu DV, Watkins MW, Kim SS, Lucovsky G. J Vac Sci Technol A 1990;8:1374.
- [15] Lee JH, Hwangbo CK. Surf Coat Technol 2000; 128–129:280.
- [16] Sen PN, Thorpe MF. Phys Rev B 1997;19:4292.
- [17] Martinet C, Devine RAB. Appl Phys Lett 1995;67:2696.
- [18] Kunio Okimura. Surf Coat Technol 2001;135:286.